nature physics

LETTERS

PUBLISHED ONLINE: 18 OCTOBER 2009 | DOI: 10.1038/NPHYS1402

X-ray astronomy in the laboratory with a miniature compact object produced by laser-driven implosion

Shinsuke Fujioka[1]*, Hideaki Takabe[1], Norimasa Yamamoto[1], David Salzmann[1], Feilu Wang[2], Hiroaki Nishimura[1], Yutong Li[3], Quanli Dong[3], Shoujun Wang[3], Yi Zhang[3], Yong-Joo Rhee[4], Yong-Woo Lee[4], Jae-Min Han[4], Minoru Tanabe[1], Takashi Fujiwara[1], Yuto Nakabayashi[1], Gang Zhao[2], Jie Zhang[3,5] and Kunioki Mima[1]

X-ray spectroscopy is an important tool for understanding the extreme photoionization processes that drive the behaviour of non-thermal equilibrium plasmas in compact astrophysical objects such as black holes[1–4]. Even so, the distance of these objects from the Earth and the inability to control or accurately ascertain the conditions that govern their behaviour makes it difficult to interpret the origin of the features in astronomical X-ray measurements. Here, we describe an experiment that uses the implosion[5] driven by a 3 TW, 4 kJ laser system[6] to produce a 0.5 keV blackbody radiator that mimics the conditions that exist in the neighbourhood of a black hole. The X-ray spectra emitted from photoionized silicon plasmas resemble those observed from the binary stars Cygnus X-3 (refs 7, 8) and Vela X-1 (refs 9–11) with the Chandra X-ray satellite. As well as demonstrating the ability to create extreme radiation fields in a laboratory plasma, our theoretical interpretation of these laboratory spectra contrasts starkly with the generally accepted explanation for the origin of similar features in astronomical observations. Our experimental approach offers a powerful means to test and validate the computer codes used in X-ray astronomy.

X-ray spectroscopy with an X-ray satellite is the main observational method to give information about compact objects, especially black holes. Black holes are indirectly studied by observing the X-ray continuum from a heated accretion disc and the X-ray fluorescence from the ambient gas of the stellar wind and the surface of a companion star in their binary systems. To derive physical properties from the observations, X-ray astronomers rely on non-local-thermodynamical-equilibrium (LTE) atomic physics in a cold ambient gas subject to an extreme radiation field, for which the mean radiation temperature is of the order of 1 keV. Theoretical models have been developed on the basis of the observed spectra[1–4] and complex computer codes were developed to analyse the observed X-ray spectra[12–16]. The underlying assumption of these models is that the spectrum originates from a photoionized plasma. In other words, the intense radiation from the compact object photoionizes the gas, and generates a relatively low-electron-temperature highly ionized non-LTE plasma. However, laboratory experiments on non-LTE photoionized plasmas have not been possible, mainly owing to the lack of an intense source of X-ray continuum radiation. Only recently has pulsed power apparatus, laser and Z-pinch, reproduced the extreme conditions in the Universe[17–20].

Here, we present a terrestrial generation and spectroscopy of non-LTE photoionized plasma. The novelty of the present experiment is the notion that a laser-driven implosion can create a flash of brilliant Planckian X-rays that can be used to simulate X-rays from a astronomical compact object. X-ray spectra with two characteristic spectral peaks were observed for a photoionized silicon plasma generated in the laboratory. This spectral shape closely resembles those observed from Cygnus X-3 and Vela X-1, as shown in Fig. 1a–c. In Fig. 1a,c, even the small bump between the two peaks is reproduced. The spectral resolution in the experiment was $\Delta h\nu = 7$ eV owing to the size of the photoionized plasma ($500 \times 500\,\mu m^2$). This resolution is similar to that of the astronomical observations in Fig. 1b,c. The error bars in the laboratory experiment originate dominantly from signal fluctuation in the three different laser shots and those in astronomy originate from photon statics. Uncertainties of the energy scale are 2 eV in the laboratory experiment and in the range between 1 and 2 eV (refs 7, 9) in the astronomical observation.

Cygnus X-3 is a well-known X-ray object identified in the early stages of X-ray astronomy[21]. It is a binary system consisting of a black-hole candidate and a companion star. A schematic of such a binary system is shown in Fig. 2a, in which the gravitational energy of the accreting material is converted into thermal energy, which is the origin of the strong radiation emitted from the accretion disc[22]. Figure 1b shows an X-ray spectrum from Cygnus X-3 observed with a spectrometer onboard the Chandra X-ray satellite. The spectrum is thought to be strongly redshifted by $800\,km\,s^{-1}$ (ref. 7). Line X-rays from highly ionized silicon ions are emitted from the surface of the companion star, the area of which is much larger than that of the accretion disc and the black hole. The electron temperature of the surface is determined to lie in the range of 5–50 eV by fitting the spectral shape of several radiative recombination continua[7,8]. This temperature is too low to ionize silicon atoms to hydrogen- and helium-like ions. This fact is direct evidence that the lines in the kiloelectronvolt range are

[1]Institute of Laser Engineering, Osaka University, 2-6 Yamada-oka, Suita, Osaka, 565-0871, Japan, [2]National Astronomical Observatories, Chinese Academy of Sciences, Beijing 100012, China, [3]Beijing National Laboratory for Condensed Matter Physics, Institute of Physics, Chinese Academy of Sciences, Beijing 1000190, China, [4]Laboratory for Quantum Optics, Korea Atomic Energy Research Institute, 1045 Daedeok Street Yuseong-gu, Daejon 305-353, Korea, [5]Department of Physics, Shanghai Jiao Tong University, Shanghai 200240, China. *e-mail: sfujioka@ile.osaka-u.ac.jp.

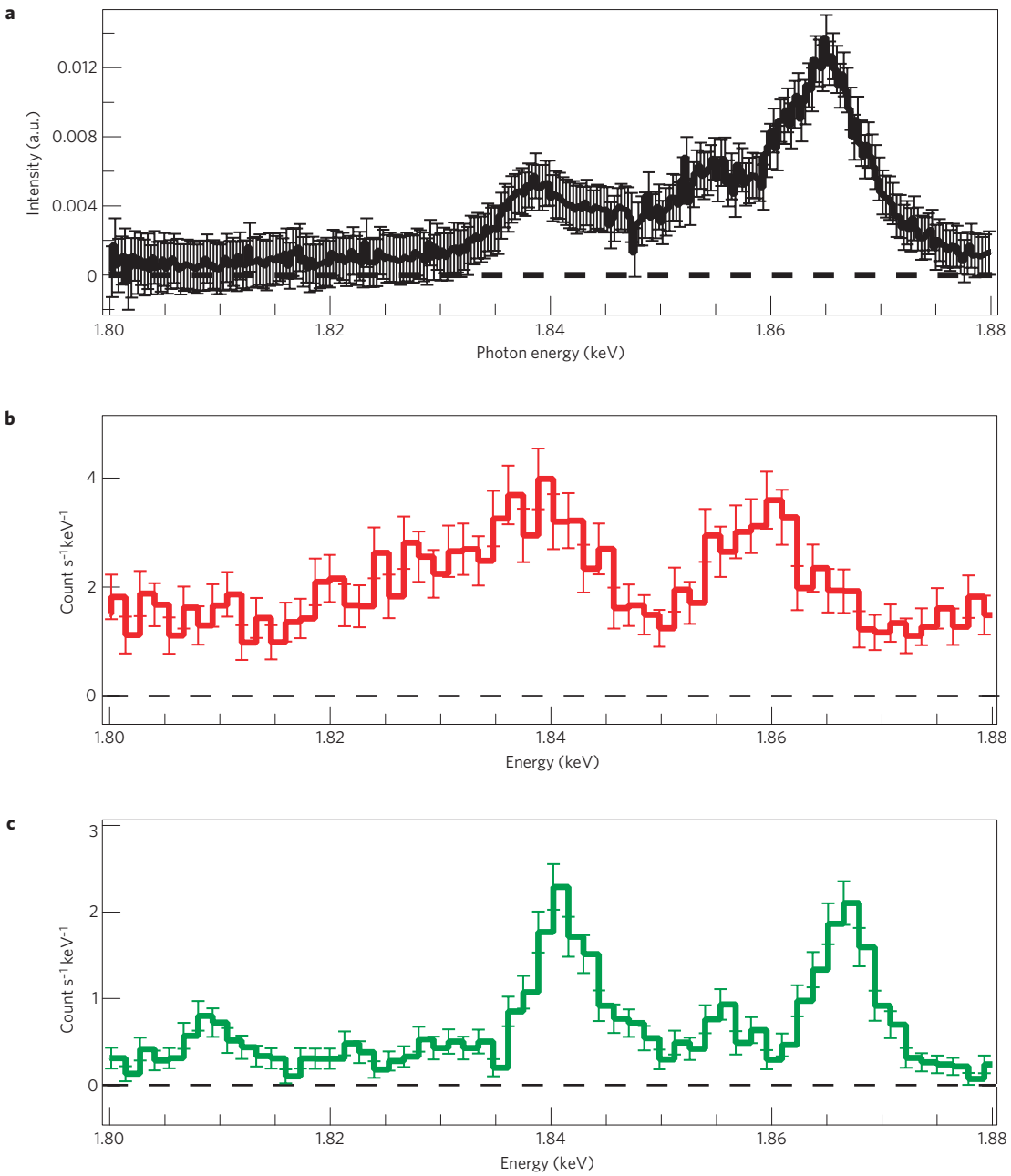

Figure 1 | Comparison of X-ray spectra observed in the laboratory and astronomy. a–c, X-ray spectrum from a photoionized plasma generated in the laboratory (**a**) and those observed from astronomical objects, Cygnus X-3 (**b**) and Vela X-1 (**c**). The emission peaks near 1.86–1.87, 1.85–1.86 and 1.84 keV are identified in astronomy to stem from resonance, intercombination and forbidden transitions of helium-like silicon ions, respectively. The spectrum from Cygnus X-3 is thought to be strongly redshifted by 800 km s^{-1}. The error bars in the laboratory experiment originate dominantly from signal fluctuation in the three different laser shots and those in astronomy originate from photon statistics. Uncertainties of the energy scale are 2 eV in the laboratory experiment and in the range between 1 and 2 eV in the astronomical observation.

due to photoionization by high-energy photons around the black hole. Similar X-ray spectra were also observed from Vela X-1, a neutron-star binary system[9–11], as shown in Fig. 1c.

A direct laser-driven implosion[5] was used to create a hot, dense plasma. A spherical hollow plastic shell, the diameter and thickness of which were respectively $505 \pm 5\,\mu m$ and $6.4 \pm 0.1\,\mu m$, was imploded by 12 beams from the GEKKO-XII laser facility[6] carrying $4.0 \pm 0.2\,kJ$ of total energy at 1.2 ± 0.1 ns green ($\lambda_L = 0.53\,\mu m$) laser pulses. The imploded core typically approaches 1 keV in temperature and $0.1\,g\,cm^{-2}$ in areal density; the areal density is high enough to be optically thick for a few kiloelectronvolt X-rays. The measured X-ray spectrum from the imploded core plasma was compared with calculated Planckian spectra modified by the spectral response of the spectrometer consisting of a transmission grating, a CCD (charge-coupled device) camera and several X-ray filters. Figure 3 shows an example of this measurement. The resulting spectrum for a 500 eV blackbody shows the best agreement with the measured one; the radiation temperature of the imploded core plasma was in the range of 480 ± 20 eV, which is consistent with a separate measurement (see the Methods section). The duration of the radiation pulse was measured with an X-ray streak camera to be 160 ± 20 ps, which is long enough to study atomic processes of interest as discussed below. As shown in Fig. 2b, a $500 \times 500\,\mu m$ square and 25-μm-thick tantalum plate, with a slit

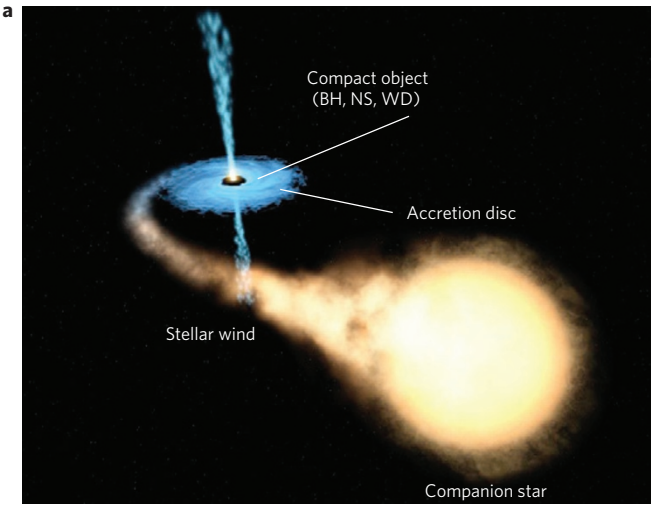

Figure 2 | Illustrations of photoionizing plasma systems in the laboratory experiment and astronomy. a, A schematic diagram of a binary system consisting of a black hole and a companion star. Ambient gases are photoionized by strong radiation emitted from the accretion disc. (These images were created for the European Space Agency by the Hubble European Space Agency Information Centre and for NASA by STScI under Contract NAS5-26555.) BH: black hole, WD: white dwarf, NS: neutron star. **b**, Schematic view of the photoionized plasma experiment. A spherical hollow plastic shell is imploded with 12 laser beams from the GEKKO-XII facility. The resulting core plasma simulates X-rays from a compact object, a Planckian X-ray radiator with a radiation temperature of 480 ± 20 eV. Silicon plasma with a 30 eV temperature was produced in the vicinity of the Planckian radiator. The angle between the line of sight of the X-ray spectrometer and the target normal is 25°.

(100 μm width and 400 μm height) in it, was inserted between the silicon plasma and the core plasma to prevent the direct illumination of X-rays from the imploded core onto the silicon surface. The distance from the centre of the slit to the silicon surface was 100 μm. A part of the silicon plasma, positioned 1.2 mm from the imploded core, was irradiated through the slit by a 500 eV Planckian spectrum with a radiation intensity $(6.5 \pm 3.5) \times 10^{-4}$ times the blackbody value. The silicon foil was heated by a second, weak infrared ($\lambda_L = 1.064\,\mu m$) laser pulse, the intensity, duration and incident angle of which were respectively $5 \times 10^{10}\,W\,cm^{-2}$, 10 ns and 10° respective to the foil normal. Consequently, a slowly expanding, cold and low-density silicon plasma mimicking astronomical ambient plasma is produced.

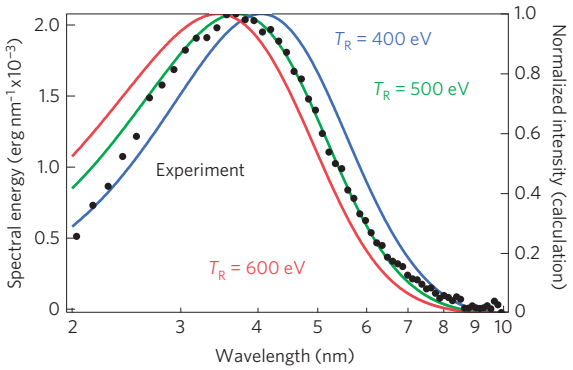

Figure 3 | X-ray spectrum from the core plasma measured with a transmission-grating spectrometer. The Planckian spectrum for 500 eV of radiation temperature shows the best agreement with the experiment after accounting for the spectral response of the spectrometer.

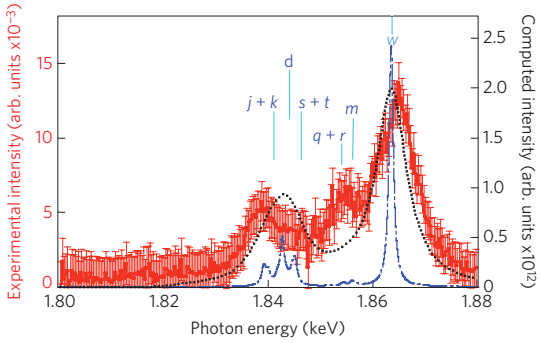

Figure 4 | Comparison between the experimental and time-integrated computed X-ray spectra from the photoionized silicon plasma. Experimental spectrum: solid line; time-integrated computed X-ray spectrum: dotted line. The fine structure of the computed spectrum (dotted line) is also shown, with key letters according to Gabriel's definition[24]. The error bars originate from signal fluctuation in the three different laser shots.

The average electron temperature and density of the preformed silicon plasma, which is located within the slit width, were $T_e = 27.5 \pm 1.5$ eV and $n_e = (0.75 \pm 0.25) \times 10^{20}\,cm^{-3}$, respectively, just before the photoionization. Suprathermal electrons emanating from the imploding plasmas and the contamination layer on the silicon surface have negligible effects on the photoionized plasma generation as discussed in the Methods section.

In the astrophysical literature[1,19], the ionization parameter is defined as $\xi = 16\pi^2 J/n_e$ (with units of erg cm s^{-1}) to measure the importance of photoionization in a plasma; here J is the mean radiation intensity per steradian, integrated over the solid angle and integrated in photon energy. In the photoionized plasma region, highly ionized ions are observed by ultraviolet and X-ray satellites over the range $\xi = 10$–10^4 ergs cm s^{-1}. In the present experiment, the ionization parameter is $\xi = 5.9 \pm 3.8$, which is only slightly below the astrophysical value.

X-ray spectra from the laboratory photoionized plasma were measured with an X-ray spectrometer using a rubidium acid phthalate crystal and an X-ray CCD camera. The preformed silicon plasma was produced before the flash of the blackbody X-ray pulse; the peak of the X-ray pulse was simultaneous with the peak of the Nd:YAG laser. The expanded silicon plasma was exposed to a continuum X-ray pulse through the slit; then the characteristic line emission around 2 keV of photon energy was clearly observed as shown in Fig. 1a. Other experimental results, described in the Methods section, also support the fact that the line X-rays are induced by photoionization.

Typical timescales of photoionization of L-shell and K-shell electrons from silicon ions are calculated to be 50 ps and 275 ps, respectively. These timescales are comparable to the duration of the radiation pulse (160 ps); thus, a time-dependent calculation of the ionization balance is crucial to clarify the physical processes that lead to the experimental spectrum by computational modelling. The computational modelling includes the simulation of the incident radiation field and its effects on the time-dependent energy- and ionization-state balance in the photoionized silicon plasma. The maximum electron temperature in computation reaches 50 eV shortly after the X-ray irradiation peaks, and slowly cools down at a later time. At such low temperatures, photoionization, radiative recombination and spontaneous decay of the excited states were identified as the dominant processes influencing the population of the ionization and excitation state distributions. The computed average ionization reaches a maximum of 11.9 shortly after the peak of the radiation pulse; later the recombination process gradually reduces it. The atomic energy levels and transition probabilities were obtained from the HULLAC code[23]. The computed time-integrated spectrum is shown in Fig. 4 (dotted line) in comparison with the experimental one. Line broadening was taken into account. The fine structure of the computed spectrum (dotted line) is also shown in Fig. 4, with key letters labelled according to Gabriel's convention[24].

The computed spectrum shows two spectral peaks: the $1s^2\ ^1S_0$–$1s2p\ ^1P_1$ resonance transition in helium-like silicon ions at 1.863 keV and a combination of three satellite lines from Li-like ions around 1.840 keV. The computations indicate that the resonance line stems from photoionization of a K-shell electron in Li-like ions followed by radiative decay of an L-electron into the K-shell vacancy. The Li-like satellite lines originate from Be-like ions by a similar mechanism. There is a significant difference in the experimental and computed spectra around 1.855 keV. Direct dielectronic satellites are unlikely, because very few electrons in a 30 eV silicon plasma can drive resonant electron capture at the silicon K-shell energy. We have carried out detailed estimates for the timescales of several possibilities to excite these doubly excited states. All of the reasonable processes turned out to have very low probabilities owing to the short time period available. Level mixing owing to local instantaneous electric field, too, could not reproduce the observed spectrum. At present, we still do not have a satisfactory explanation for this bump.

We obtained X-ray spectra in the laboratory that resemble those observed astronomically, although their interpretations are contradictory. The spectral peaks near 1.86 and 1.84 keV in Fig. 1b,c are thought to be a resonance line ($1s^2\ ^1S_0$–$1s2p\ ^1P_1$) and a forbidden one ($1s^2\ ^1S_0$–$1s2s\ ^3S_1$) of helium-like silicon ions in astronomy[9]. The emission lines in Fig. 1a,b are not aligned in energy, and they do not seem to be simply redshifted by 800 km s^{-1} relative to the laboratory spectrum. There may be a differential Doppler shift for the resonance and forbidden lines, otherwise, the line identification is questionable in Fig. 1b.

The HULLAC code indicates that the forbidden line of helium-like silicon ions should occur at 1.84 keV. This photon energy is coincidentally almost equal to that of the satellite lines, but the transition probability of the forbidden line is 10^{-8} times smaller than that of the resonant line. Consequently, the population of the $1s2s$ state must be 10^8 times larger than that of the $1s2p$ state, if the peaks near 1.84 keV do in fact stem from the forbidden transition. We have estimated the timescales of several possible mechanisms that could generate an overpopulation of the $2s$ metastable state. All of these timescales turned out to be much longer than the lifetime of the laboratory photoionized plasma. It therefore seems difficult to believe that electrons accumulated in the $1s2s$ state in the present experiment. Nevertheless, it is still too early to make conclusions about the origin of the 1.84 keV peak in the astronomical case, because the radiation flux is pulsed in the laboratory but continuous from compact objects. It is worth noting that the Li-like satellite lines, which are generated from Be-like species by photoionization, should be incorporated also in the analysis of astronomical spectra.

Methods

Measurement of radiation temperature of imploded core plasma. X-ray continua from imploded core plasma were characterized with two types of X-ray spectrometer, one is an absolutely calibrated transmission-grating spectrometer and the other is a filtered-pinhole-array one. These were coupled with cooled X-ray CCD cameras, in which the spectral response and analog-to-digital conversion gain were calibrated with two radio isotopes (^{55}Fe and ^{109}Cd) that emit 3-, 6- and 22-keV X-rays. The transmission-grating spectrometer was designed to measure the absolute intensity and spectral shape of the core plasma in the photon-energy range of 1–6 keV, and the filtered-pinhole-array spectrometer was designed to obtain the two-dimensional distribution of the radiation temperature (T_R) with nine X-ray filters covering the photon-energy range of 1–8 keV.

Effects of hydrocarbon contamination layer on silicon foil. The source of the preformed silicon plasma was 1-μm-thick silicon coated on a 25-μm-thick plastic sheet, the surface of which may be contaminated dominantly by hydrocarbon (CH_2, $\rho = 1$ g cm^{-3}) originated from ambient air. The thickness of the contamination layer depends both on the treatment of the target surface and the properties of the vacuum system; for example, the thickness of the contamination layer on a gold target is reported to be 1.2 nm (ref. 25). Even if the surface of the silicon target was covered with a 10 nm hydrocarbon layer, such a contamination layer is ablated within 0.75 ns, as evaluated by a scaling law[26,27], by a 1.064 μm wavelength and 5×10^{10} W cm^{-2} intensity Nd:YAG laser pulse. The hydrocarbon plasma expands at 4.5×10^6 cm s^{-1}, which is the velocity of sound in a 30 eV hydrocarbon plasma. The contamination layer moved to 190 μm from the surface at the photoionization timing. Thus, a nearly pure silicon plasma is photoionized in the experiment.

Measurement of electron temperature and density of preformed silicon plasma. The electron temperature (T_e) and number density (n_e) of the preformed silicon plasma were evaluated by extreme-ultraviolet spectroscopy coupled with the collisional-radiative code FLYCHK (ref. 15). The target used in this measurement is the same one used in the photoionized plasma generation, a slit (with a 100 μm width and 400 μm height) in a tantalum plate attached to a silicon target. The distance from the centre of the slit to the target surface was 100 μm along the target normal. Extreme-ultraviolet light was observed through the slit with a grazing-incidence spectrometer, for which the line of sight was parallel to the silicon surface. The evaluated electron temperature and density are average values of the plasma located within the slit width. The spectrum was recorded on an X-ray streak camera, for which the temporal resolution was about 1 ns. The measured extreme-ultraviolet spectrum consists of many lines from Si^{6-8+} ions. Root-mean-square differences between the measured spectrum and calculations for various electron temperatures and densities indicate that those of the preformed silicon plasma are in the range of $T_e = 26$–29 eV and $n_e = (0.5$–$1.0) \times 10^{20}$ cm^{-3}, respectively, just before being illuminated by radiation emission from the implosion core.

Effects of suprathermal electrons emanated from imploding plasmas. The generation of suprathermal electrons in the interaction of intense laser radiation with an imploding plasma is the considerable difference between the experimental system and the astronomical one. In a previous experiment[28] in which the conditions were similar to those in the present experiment, a plastic foil was irradiated by a 0.53 μm wavelength laser with an intensity of 2×10^{15} W cm^{-2}; then 10^{-4} of the laser energy was converted into the suprathermal electrons with a broad spectrum having 50 keV of slope temperature. In spite of the fact that the suprathermal electron transport is rather complex as a consequence of refluxing in the plasma sheath and surface transport, the increment of electron temperature is only 2.9 eV, even if all of the incident suprathermal energy is thermalized in the photoionized plasma region ($100 \times 400 \times 500$ μm^3 in volume). This evaluation indicates that suprathermal electrons have a negligible effect on atomic kinetics in the laboratory photoionized plasma.

Validation experiment of photoionized plasma generation. To validate the photoionized plasma production, three types of laser shot were carried out. In the first shot, only a preformed silicon plasma was produced; the temperature of the preformed Si plasma was too low (~30 eV) to radiate kiloelectronvolt X-rays, and thus no X-ray signal was detected on the spectrometer. In the second shot, a silicon target was not irradiated with the Nd:YAG laser, and only an imploded core plasma was created. In this case, there was no silicon plasma along the X-ray path limited by the slit; thus, the X-ray spectra had a low intensity. In the third shot, the preformed silicon plasma was produced before the flash of the blackbody X-ray pulse; the peak of the X-ray pulse was simultaneous with the peak of the Nd:YAG laser. The

expanded silicon plasma was exposed to a continuum X-ray pulse through the slit; then the characteristic line emission around 2 keV of photon energy was clearly observed, as shown in Fig. 1a. Note that emission intensities were sensitive to the delay between the flash of the blackbody radiation and the peak of the Nd:YAG laser pulse. The delay was varied to be −5, 0 and +10 ns; an intense signal was obtained in the case of 0 ns. This result also supports the fact that the line X-rays in the kiloelectronvolt energy range are induced by photoionization.

Received 5 January 2009; accepted 25 August 2009; published online 18 October 2009; corrected online 22 October 2009

References

1. Tarter, C. B., Tucker, W. H. & Salpeter, E. E. The interaction of x-ray sources with optically thin environments. *Astrophys. J.* **156,** 943–951 (1969).
2. Osterbrock, D. E. *Astrophysics of Gaseous Nebulae and Active Galactic Nuclei* (University Science Books, 1989).
3. Liedahl, D. A. *X-ray Spectroscopy in Astrophysics* 189 (Springer-Verlag, 1999).
4. Ballantyne, D. R., Ross, R. R. & Fabian, A. C. Soft x-ray emission lines from photoionized accretion discs: Constraints on their strength and width. *Mon. Not. R. Astron. Soc.* **336,** 867–872 (2002).
5. Nuckolls, J., Wood, L., Thiessen, A. & Zimmerman, G. B. Laser compression of matter to super-high densities: Thermonuclear (CTR) applications. *Nature* **239,** 139–142 (1972).
6. Yamanaka, C. *et al.* Nd-doped phosphate glass laser systems for laser-fusion research. *IEEE J. Quantum Electron.* **QE-17,** 1639–1649 (1981).
7. Paerels, F. *et al.* High-resolution spectroscopy of the x-ray-photoionized wind in cygnus x-3 with the chandra high-energy transmission grating spectrometer. *Astrophys. J.* **533,** L135–L138 (2000).
8. Liedahl, D. A. & Paerels, F. Photoionization driven x-ray line emission in cygnus x-3. *Astrophys. J.* **468,** L33–L36 (1996).
9. Schulz, N. S., Canizares, C. R., Lee, J. C. & Sako, M. The ionized stellar wind in vela x-1 during eclipse. *Astrophys. J.* **564,** L21–L25 (2002).
10. Goldstein, G., Huenemoerder, D. P. & Blank, D. Variation in emission and absorption lines and continuum flux by orbital phase in vela x-1. *Astron. J.* **127,** 2310–2321 (2004).
11. Watanabe, S. *et al.* X-ray spectra study of the photoionized stellar wind in vela x-1. *Astrophys. J.* **651,** 421–437 (2006).
12. Kallman, T. R., Liedahl, D., Osterheld, A., Goldstein, W. & Kahn, S. Photoionization equilibrium modeling of iron L line emission. *Astrophys. J.* **465,** 994–1009 (1996).
13. Ferland, G. J. *et al.* CLOUDY 90: Numerical simulation of plasmas and their spectra. *Publ. Astron. Soc. Pacif.* **110,** 761–778 (1998).
14. Rose, S. J. The non-LTE excitation/ionization code GALAXY. *J. Phys. B* **31,** 2129–2144 (1998).
15. Chung, H. K., Chen, M. H., Morgan, W. L., Ralchenko, Y. & Lee, R. W. FLYCHK: Generalized population kinetics and spectral model for rapid spectroscopic analysis for all elements. *High Energy Density Phys.* **1,** 3–12 (2005).
16. Rose, S. J. *et al.* Calculation of photoionized plasma with an average-atom model. *J. Phys. B* **37,** L337–L342 (2004).
17. Remington, B. A., Arnett, D., Drake, R. P. & Takabe, H. Modeling astrophysical phenomena in the laboratory with intense lasers. *Science* **284,** 1488–1493 (1999).
18. Remington, B. A., Drake, R. P. & Ryutov, D. D. Experimental astrophysics with high power lasers and Z pinches. *Rev. Mod. Phys.* **78,** 755–807 (2006).
19. Foord, M. E. *et al.* Charge-state distribution and doppler effect in an expanding photoionized plasma. *Phys. Rev. Lett.* **93,** 055002 (2004).
20. Wang, F. *et al.* Experimental evidence and theoretical analysis of photoionized plasma under x-ray radiation produced by an intense laser. *Phys. Plasmas* **15,** 073108 (2008).
21. Giacconi, R., Gorenstein, P., Gursky, H. & Waters, J. R. An X-ray survey of the cygnus region. *Astrophys. J.* **148,** L119–L127 (1967).
22. Shakura, N. I. & Sunyaev, R. A. Black holes in binary systems. Observational appearance. *Astron. Astrophys.* **24,** 337–355 (1973).
23. Bar-Shalom, A., Oreg, J. & Klapisch, M. Collisional radiative model for heavy atoms in hot non-local-thermodynamical-equilibrium plasmas. *Phys. Rev. E* **56,** R70–R73 (1997).
24. Gabriel, A. H. Dielectronic satellite spectra for highly charged helium-like ion lines. *Mon. Not. R. Astron. Soc.* **160,** 99–119 (1972).
25. Allen, M. *et al.* Direct experimental evidence of back-surface ion acceleration from laser-irradiated gold foil. *Phys. Rev. Lett.* **93,** 265004 (2004).
26. Ng, A. *et al.* Ablation scaling in steady-state ablation dominated by inverse-bremsstrahlung absorption. *Appl. Phys. Lett.* **45,** 1046–1048 (1984).
27. Fujioka, S. *et al.* Properties of ion debris emitted from laser-produced mass-limited tin plasmas for extreme ultra-violet light source application. *Appl. Phys. Lett.* **87,** 241503 (2005).
28. Rousseaux, C., Amiranoff, F., Labaune, C. & Matthieussent, G. Suprathermal and relativistic electrons produced in laser-plasma interaction at 0.26, 0.53, and 1.05 micron laser wavelength. *Phys. Fluids* **B4,** 2589–2595 (1992).

Acknowledgements

The authors would like to acknowledge the dedicated technical support by the staff at the GEKKO-XII facility for the laser operation, target fabrication, and plasma diagnostics. We also acknowledge K. Masai of Tokyo Metropolitan University and T. Dotani of the Japanese Aerospace Exploration Agency, as well as their colleagues, for valuable discussions of photoionized plasma in astronomy. This research was partially supported by the Japanese Ministry of Education, Science, Sports, and Culture (MEXT), Special Education and Research Expenses for 'Laboratory Astrophysics with High-Power Laser' and Grant-in-Aid for Young Scientists (A) for 'Non-LTE Photoionized Plasma Generation with Laser-Produced Blackbody Radiator (Grant No. 21684034)', and by the National Basic Research Program of China (973 Program, Grant No. 2007CB815102-03).

Author contributions

S.F. is the principal investigator who proposed and organized the experiment. H.T. is the leader of a project for laboratory astrophysics in ILE. Experimental data were analysed by S.F., N.Y., Q.D., S.W. and Y.Z. Theoretical analysis was carried out by D.S. and F.W. All authors contributed to diagnostics preparation, experiment and discussion of the results. The success of the study was aided by the international nature of the collaboration, in which the authors from Japan, China and Korea all contributed. This collaboration was promoted by H.T., H.N. (Japan), Y.L., G.Z., J.Z. (China) and Y.J.R. (Korea).

Additional information

Reprints and permissions information is available online at http://npg.nature.com/reprintsandpermissions. Correspondence and requests for materials should be addressed to S.F.